Journal of Dental Research
2015, Vol. 94(12) 1668–1675

DOI: 10.1177/0022034515598135
jdr.sagepub.com

Chondrocytes Directly Transform into Bone Cells in Mandibular Condyle Growth

Y. Jing[1*], X. Zhou[2*], X. Han[3], J. Jing[1], K. von der Mark[4], J. Wang[1], B. de Crombrugghe[2], R.J. Hinton[1], and J.Q. Feng[1]

Abstract

For decades, it has been widely accepted that hypertrophic chondrocytes undergo apoptosis prior to endochondral bone formation. However, very recent studies in long bone suggest that chondrocytes can directly transform into bone cells. Our initial in vivo characterization of condylar hypertrophic chondrocytes revealed modest numbers of apoptotic cells but high levels of antiapoptotic *Bcl*-2 expression, some dividing cells, and clear alkaline phosphatase activity (early bone marker). Ex vivo culture of newborn condylar cartilage on a chick chorioallantoic membrane showed that after 5 d the cells on the periphery of the explants had begun to express *Col1* (bone marker). The cartilage-specific cell lineage–tracing approach in triple mice containing Rosa $26^{tdTomato}$ (tracing marker), 2.3 $Col1^{GFP}$ (bone cell marker), and aggrecan Cre^{ERT2} (onetime tamoxifen induced) or *Col10*-Cre (activated from E14.5 throughout adult stage) demonstrated the direct transformation of chondrocytes into bone cells in vivo. This transformation was initiated at the inferior portion of the condylar cartilage, in contrast to the initial ossification site in long bone, which is in the center. Quantitative data from the *Col10*-Cre compound mice showed that hypertrophic chondrocytes contributed to ~80% of bone cells in subchondral bone, ~70% in a somewhat more inferior region, and ~40% in the most inferior part of the condylar neck ($n = 4$, $P < 0.01$ for differences among regions). This multipronged approach clearly demonstrates that a majority of chondrocytes in the fibrocartilaginous condylar cartilage, similar to hyaline cartilage in long bones, directly transform into bone cells during endochondral bone formation. Moreover, ossification is initiated from the inferior portion of mandibular condylar cartilage with expansion in one direction.

Keywords: osteoblast, osteocyte, temporomandibular joint, cell lineage tracing, development, cell transformation

Introduction

The mandibular condylar cartilage (MCC) is a principal locus at which growth of the mandible in length and height takes place. Although there is no secondary ossification center as in the primary cartilaginous growth centers of the limbs, proliferation of cells in the superficial layers of the MCC combined with endochondral bone formation at the interface of the cartilage with the subchondral bone produces new bone that directly determines the dimensional structure of the mandible. This new bone formation has long been assumed to occur similarly to the limbs: cell death of the deepest hypertrophic chondrocytes (HCs), then invasion of cells from the underlying bone marrow that erode the calcified cartilage and initiate angiogenesis, followed by cells that deposit new bone (Gibson 1998; Kronenberg 2003). Yet a number of researchers have argued for the ability of HCs to transdifferentiate, specifically into bone cells (Kahn and Simmons 1977; Roach 1992). Very recently, several reports in limb cartilages have shown that a significant proportion of the cells that contribute to new bone formation at the cartilage-bone interface originate from cells in cartilage. Enishi and coworkers (2014) found that insertion of a filter blocking vascular invasion into the hypertrophic zone of the rabbit distal ulna growth plate caused the HCs to proliferate and transform into bone cells. Using cell lineage–tracing methodologies, other groups have demonstrated that HCs are capable of changing their phenotype into bone-forming cells such as osteoblasts or even osteocytes (Ono et al. 2014; G. Yang et al. 2014; L. Yang et al. 2014; Zhou et al. 2014).

The MCC does not develop a secondary ossification center as in long bones, and it is considered a secondary cartilage; as such, it has significant developmental and structural differences from primary cartilages, such as limb growth plate and synchondroses of the head (Silbermann et al. 1987; Luder et al. 1988). In this study, we attempted to investigate whether the direct transformation of chondrocytes into bone cells occurs in

[1]Department of Biomedical Sciences, Texas A&M Baylor College of Dentistry, Dallas, TX, USA
[2]Department of Genetics, The University of Texas MD Anderson Cancer Center, Houston, TX, USA
[3]State Key Laboratory of Oral Diseases, West China Hospital of Stomatology, Sichuan University, China
[4]Department of Experimental Medicine 1, Nikolaus-Fiebiger-Center of Molecular Medicine, University of Erlangen-Nuremberg, Erlangen, Germany
[*]Authors contributing equally to this work.

A supplemental appendix to this article is published electronically only at http://jdr.sagepub.com/supplemental.

Corresponding Authors:
R.J. Hinton and J.Q. Feng, Department of Biomedical Sciences, Texas A&M Baylor College of Dentistry, 3302 Gaston Ave, Dallas, TX 75246, USA.
Email: bhinton@bcd.tamhsc.edu; jfeng@bcd.tamhsc.edu

the process of mandibular condylar bone formation. Our evaluation of the assumption that HCs undergo rampant cell death demonstrated it to be unfounded. Using cell lineage–tracing techniques, we identified numerous chondrocyte-derived bone cells in subchondral bone underlying the MCC, in condylar neck bone region, and even in periosteum. Furthermore, we quantified the number of these chondrocyte-derived cells in the condylar neck, which displayed a contribution gradient with the subchondral bone highest (~80%) and the inferior portion of the condylar neck the lowest (~40%). Finally, we demonstrated that ossification of endochondral bone formation in the condylar neck proceeds from the inferior to the superior region of the MCC, in contrast to the ossification process in long bone, which takes place in both proximal and distal directions.

Methods and Materials

Breeding Transgenic Mice

To generate triple mice for cell lineage studies of the fate of the embryonic chondrocytes in condylar bone formation, the *Col10a1-Cre* mice (Gebhard et al. 2008), *2.3Col1-GFP* mice (Kalajzic et al. 2002), and *ROSA*$^{-tdTomato}$ (B6;129S6-*Gt(ROSA)26Sor*$^{tm9(CAG-tdTomato)Hze}$/J, stock number: 009705; Jackson Laboratory, Bar Harbor, ME, USA) were internally crossed 3 times. For studies of the fate of the postnatal chondrocytes, the triple mice of Agc1-Cre^{ERT2} (Akiyama et al. 2005; Henry et al. 2009), 2.3*Col1*-GFP, and *Rosa26-*^{tdTomato} were generated first and followed by onetime tamoxifen induction at day 14 (1.5 mg/10 g of body weight). The tamoxifen (T5648; Sigma-Aldrich, St. Louis, MO, USA) was dissolved in 10% ethanol and 90% corn oil (C8267; Sigma-Aldrich). For cell proliferation analyses, bromodeoxyuridine (BrdU) (10 mL/g; Sigma-Aldrich) was injected into mice 2 times (24 and 2 h before sacrifice).

All protocols were reviewed and approved by the Institutional Animal Care and Use Committee at Texas A&M Baylor College of Dentistry.

Chick Chorioallantoic Membrane Assay

The chick chorioallantoic membrane (CAM) assays are widely used to study angiogenesis (Richardson and Singh 2003), tumor cell invasion, and metastasis (Zhai et al. 2007) and for early cartilage explant and hormone studies (Kahn and Simmons 1977; Feng and Clark 1994). Briefly, fertilized white leghorn chicken eggs were obtained from the agriculture farm of Texas A&M University. Eggs were then incubated at 37 °C with 60% humidity. A small window was made in the shell on day 3 of chick embryo development under aseptic conditions. The window was resealed with parafilm, and eggs were returned to the incubator until day 6. For obtaining cartilage explants under aseptic conditions, mandibular condyles were removed from newborn mice with dissection scissors and No. 5 forceps. After the perichondrium, periosteum, and subchondral bone were carefully removed under stereomicroscope, ~1.5-mm-long MCC explants were grafted directly onto the CAM for 5 d (see Ex Vivo Condylar Cartilage Explants on CAM Culture section).

Immunohistochemistry, Toluidine Blue, Safranin O Staining, and Alkaline Phosphatase Activity

Mandibular condyles were fixed in 4% paraformaldehyde and decalcified at 4 °C, followed by either CryoJane frozen sections as previously described (Jiang et al. 2005) or embedded in paraffin, sectioned, and stained with safranin O (proteoglycans) or toluidine blue stain (Zhang et al. 2011) or the following antibodies: rabbit polyclonal anti-Col1 (1:50; Abcam, Cambridge, England), mouse anti-Col2 monoclonal antibody (1:50; Santa Cruz Biotechnology, Dallas, TX, USA), and rabbit polyclonal anti-Bcl2 (B-cell lymphoma 2, 1:50; Abcam). Detection of immunoreactivity for all preparations was done by 3,3-diaminobenzidine kit (Vector Laboratories, Burlingame, CA, USA). The detection for BrdU was done by kit from Invitrogen (93-3944; Waltham, MA, USA). TUNEL was detected by kit from Millipore (S7100; Temecula, CA, USA). Alkaline phosphatase (ALP) enzyme activity was measured in tissue slides using an ALP Assay Kit (Roche, Indianapolis, IN, USA).

Confocal Microscope and Statistical Analyses

Fluorescent cell images were captured using an SP5 Leica confocal microscope. All images were captured at wavelengths ranging from 488 (green) to 561 (red) μm. Multiple stacked images were taken at 200 Hz (dimension, 1,024 × 1,024). In 4 mice, the number of red, yellow, and green bone cells (osteoblasts and osteocytes) was manually counted in an area measuring 700 × 600 × 10 μm in 3 regions (superior, middle, and inferior) of the condylar process. For each region, the Kruskal-Wallis test was used to detect any significant differences among samples. The Mann-Whitney *U* test (post hoc test) was used to compare differences among the 3 regions.

Results

Characteristics of HCs

To examine the assumption that the deepest layers of HCs enter apoptosis as a prelude to deposition of new bone, we investigated the status of the cell cycle (cell division and death) by analyzing immunoreactivity of these cells to BrdU (cell division), apoptotic factor (TUNEL), and antiapoptotic factor (Bcl2) at the rapid growth ages of postnatal days 1 and 10 (P01 and P10). As expected, at P01 and P10, BrdU-labeled cells were located primarily in the articular disc, prechondroblastic layer of the MCC, and the subchondral bone; the number of labeled cells was somewhat attenuated in all locations at P10. However, some dividing cells were visible in the lower layers of HCs at both ages (Fig. 1a, P01; Fig. 1b, P10).

Next, we studied the cell death status of HCs. At birth, TUNEL staining for apoptotic cells showed a roughly equal number of apoptotic cells in the HC and the subchondral bone

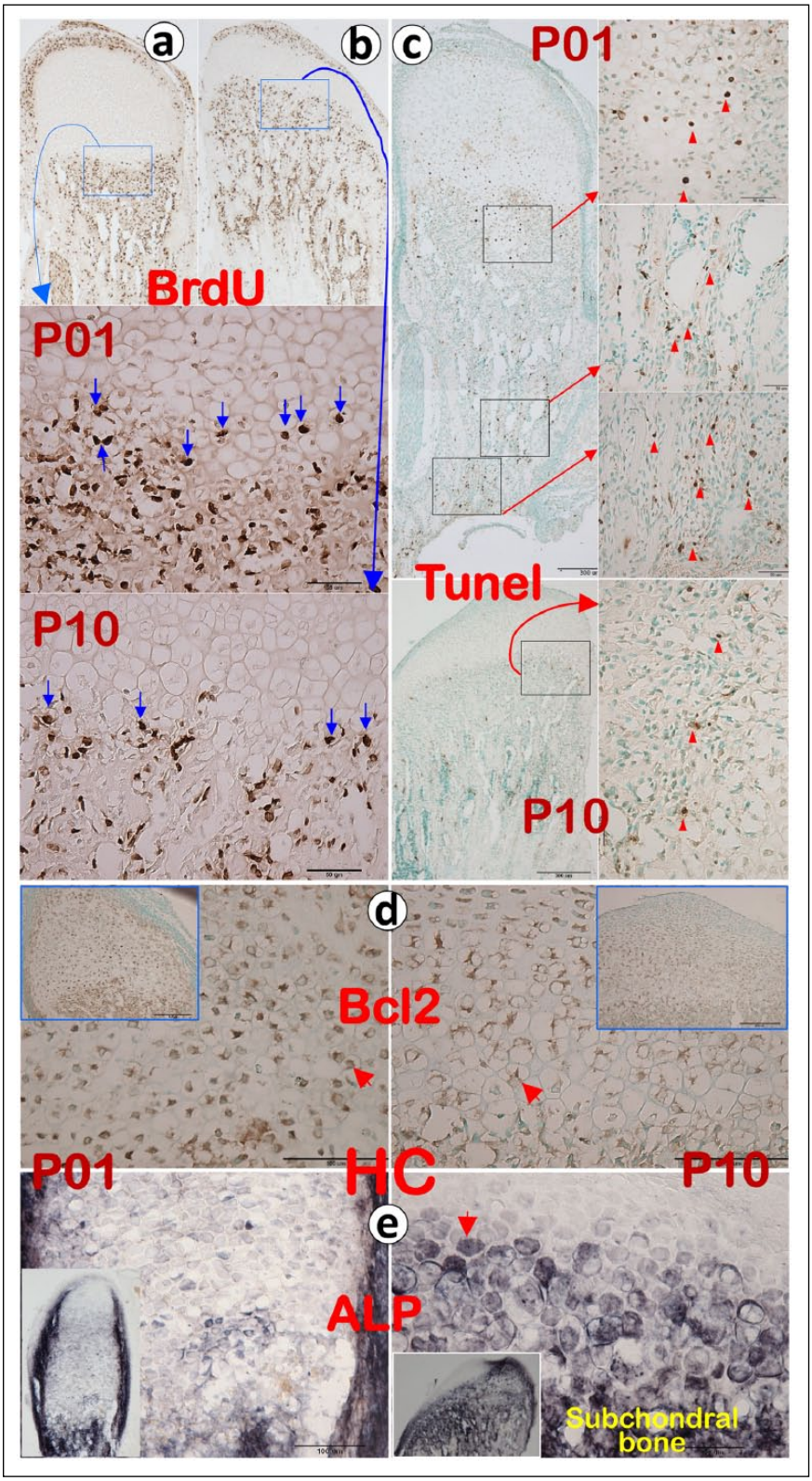

Figure 1. There are few TUNEL (apoptotic)–positive hypertrophic chondrocytes (HCs) but abundant Bcl-2 (B-cell lymphoma 2, a critical antiapoptotic factor)–positive HCs, which maintain a high activity of alkaline phosphatase (ALP; an early osteoblast marker) with some cell division. Anti-BrdU immunostaining images display a higher number of proliferating cells at postnatal day 1 (P01, blue arrows) (**a**) than those at P10 (**b**; blue arrows), including some BrdU-positive dividing cells in HC zone. (**c**) TUNEL immunostaining assay showed more positively stained HCs and bone cells (red arrowheads) at postnatal day 1 (P01; upper panel) than at P10 (lower panel). (**d**) Anti-Bcl-2 immunostained images showed that the Bcl-2-positive mature chondrocytes (brown, red arrows) were found in the entire HC zone at both P01 (left panel) and P10 (right panel). (**e**) ALP activity was detected in most chondrocytes at P01 (left panel, red arrows) and remained active mainly in mature chondrocytes at P10 (right panel). In addition, ALP was detected in all progenitor cells in perichondrium and periosteum at both developmental stages.

cells (Fig. 1c). The number of apoptotic cells was considerably reduced at P10 in both locations. Immunoreactivity for Bcl2 was strong in chondrocytes from all layers of the MCC at both P0 and P10 ages (Fig. 1d).

It has been known for a long time that HCs express ALP, although it was puzzling why the dying HCs produced the early bone marker. We found that ALP staining was prominent intracellularly in HCs in the MCC at both P01 and P10 (Fig. 1e). Furthermore, periosteal and perichondrial cells showed strong immunoreactivity for ALP in condyle.

The above cell cycle, Bcl2, and ALP data strongly support the notion that the most HCs are not dying cells as commonly believed and that these cells may serve as precursor cells for bone cells during endochondral bone formation.

Ex Vivo Condylar Cartilage Explants on CAM Culture

To further examine the possibility that MCC chondrocytes transform to bone cells independent from the potential impact of systemic factors, we took the newborn condyle cartilage and did 5-d cartilage explant culture using the CAM model (Fig. 2a). Hematoxylin and eosin– and toluidine blue–stained images showed bonelike matrix and osteoblast-like cells (Fig. 2b). Furthermore, strong immunoreactivity for Col I was apparent on the surfaces of the condyle explant with Col II immunoreactivity in the explant center (Fig. 2c).

Cell Lineage–tracing Technique Shows Chondrocyte Transformation

To definitively establish whether chondrocytes directly transform into bone cells and to determine the relative contribution of chondrocytes and non-chondrocytes to producing bone cells in the MCC, we employed cell lineage–tracing techniques. To facilitate understanding of this approach, we created a cartoon (Fig. 3a) to show the role of each mouse line. For example, the 2.3Col 1-GFP line gives rise to green-fluorescing color, representing bone cells (Fig. 3b), while the cross between the Agr (aggrecan)-Cre^{ERT2} line (or *Col* 10-Cre; not shown) and Rosa26-^{tdTomato} line together will activate red tomato reporter in all chondrocytes and the cells derived from chondrocytes (Fig. 3c). Furthermore, when all mouse lines are bred together, the red and green colors are superimposed, leading to yellow fluorescence (combination of red and green; Fig. 3d). This is indicative of chondrocytes (red) that have transformed to bone cells and are expressing *Col 1* (green). A similar appearance to that seen in articular cartilage is evident for the mandibular condyle (Fig. 3e), in which the trabecular bone just deep to the cartilage contains a mixture of red, yellow, and green cells, with red predominating; this mixture persists deeper into the ramus, gradually changing as green becomes the predominant color.

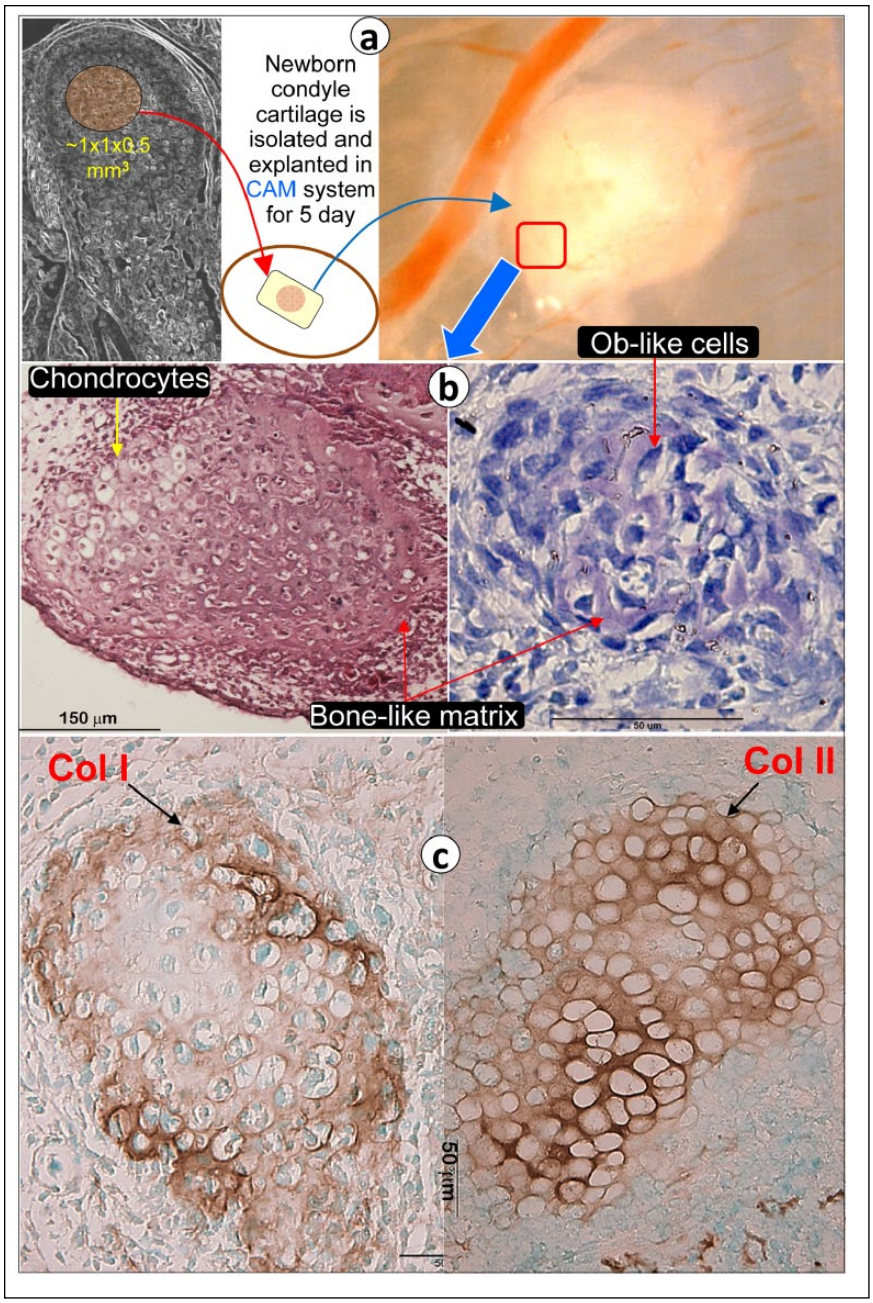

Figure 2. Chondrocytes from condylar cartilage are transformed into bonelike cells in chorioallantoic membrane (CAM) culture. (**a**) Newborn condylar cartilage (with perichondrium, periosteum, and subchondral bone removed) was cultured on the CAM for 5 d. (**b**) The hematoxylin and eosin– and Toluidine blue–stained images revealed that bonelike matrix and osteoblast (Ob)–like cells were evident.(**c**) Antipolyclonal immunostaining images revealed strong Col I immunoreactivity (left) on the periphery of the condyle explant with Col 2 immunoreactivity in the explant center (right), indicating a cartilaginous phenotype transforming to an osteoblastic phenotype.

Differential Derivation of Bone Cells in Subchondral Bone by Depth

To precisely define the bone cell origin in different regions of the ramus inferior to the MCC during development, we arbitrarily selected 3 equal-sized regions designated as S (superior, adjacent to the cartilage-bone interface, extending inferiorly approximately 600 µm), M (middle), and I (inferior, just superior to the root of the lower incisor) at the age of P21 (Fig. 4d, upper left and entire right panels) with the enlarged views shown in Appendix Figure 2. Differences in the distribution of cells by color were quantitatively compared among the 3 regions (Fig. 4d, lower left). In the superior region, only about 20% of cells fluoresced green, meaning that around 80% of the cells in this region of bone were chondrocytic in origin (red, yellow). The middle region contained around 70% cells of chondrocytic origin, while in the inferior region, cells of chondrocytic origin were around 40%. Significant ($P < 0.01$) differences in the percentage of red, yellow, and green cells were present between the superior/middle groups and the inferior group; no significant percentage differences were detected between the superior and middle regions.

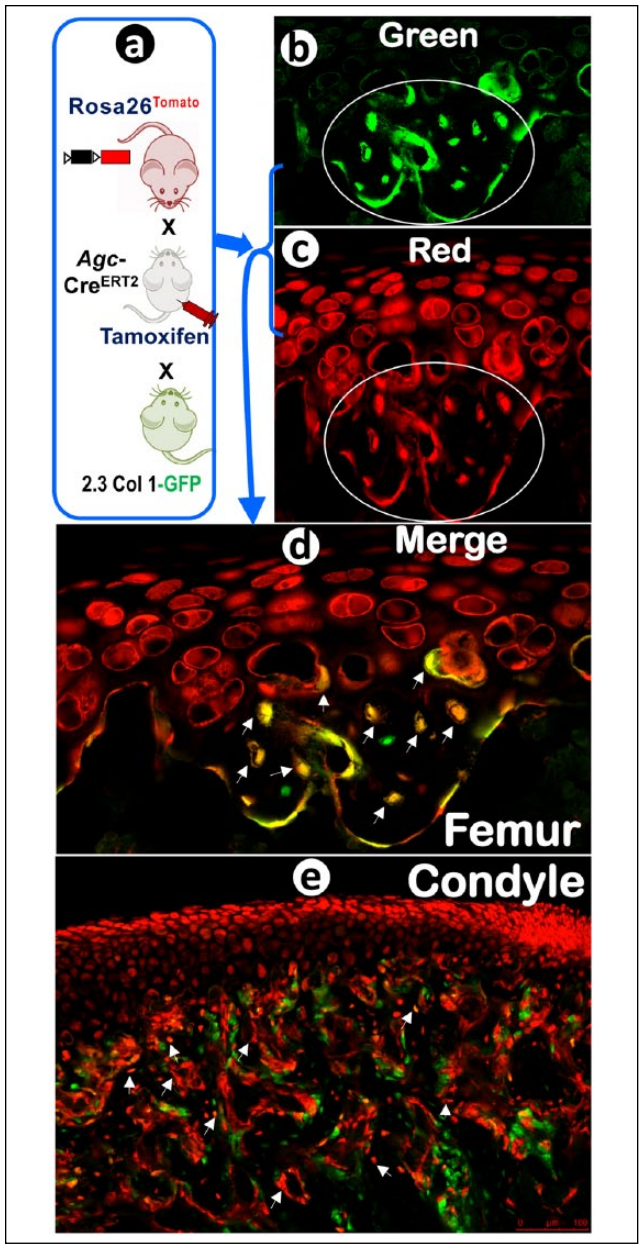

Figure 3. Cellular colocalization of the chondrocyte-derived tomato marker and a 2.3 *Col1*-GFP osteoblast-specific marker in femur and condylar subchondral bone sections of *Aggrecan (Agc)-Cre* ^{ERT2}*, 2.3Col1-GFP, ROSA-*^{tdTomato} triple transgenic mice. (**a**) A cartoon illustrating the cross that generates triple mice containing *Agc-Cre*^{ERT2}*, ROSA-*^{tdTomato}, and *2.3Col1-GFP*, with tamoxifen induction at postnatal day 14 (P14) and harvest at P28 for confocal imaging. Confocal images from green channel (**b**), red channel (**c**), and merged channels (**d**; white arrows) in femur. These long bone data are provided for comparison with the mandibular condyle data in panel e. (**e**) Merged image of the mandibular condyle obtained from the same age mouse as in panels b to d showed abundant Tomato-positive chondrocytes (red) and bone cells (red and yellow) throughout the subchondral bone area with few green bone cells, which are derived from nonchondrocyte progenitor cells.

Cell Lineage–tracing Technique Shows Site and Direction of MCC Ossification

To our knowledge, the initiation site and direction of ossification during condylar endochondral bone formation have not been well defined. To address this fundamental question, we generated a similar triple mouse line as shown in Figure 3a, except that the Agr-Cre^{ERT2} line was replaced by the *Col 10*-Cre, in which the Cre is activated at E14.5 and continues throughout development (Fig. 4a, left). The development of the bone deep to the MCC can be examined by comparing the condyle and ramus from P0 with that in P10 (Fig. 4a, right) and late stage (see below). At P0, most of the cells in the bone directly deep to the carrot-shaped MCC are red with very few yellow, indicating transformation from the initial chondrocytes into bone cells (Fig. 4b). This finding also indicates that the initial ossification site started from the inferior portion of MCC. Because virtually all of the cells in the periosteum and perichondrium are green, the green bone cells in these areas are not derived from chondrocytes. By P10, the condyle has begun to assume a more mushroom-shaped morphology (Fig. 4c). Green cells are in a distinct minority in the trabeculae near the cartilage-bone interface, where red and some yellow cells predominate. In the trabeculae just deep to this area, yellow cells are in the majority, along with many red cells. Green cells appear to be in the majority only in the most inferior trabeculae (see lower inset). The cortical bone of the ramus (composed of numerous yellow cells) and the marrow cavity has formed with many chondrocyte-derived marrow cells (red). The periosteum and its extension, the perichondrium, continue to be composed almost completely of green cells.

To further investigate the initial site of ossification, we generated the compound mice containing Rosa26-^{tdtomato} and *Col10*-Cre lines (Appendix Fig. 1a), followed by collections of E16.5 and 18.5 condyles for analyses of confocal and toluidine-blue images. At E16.5, the condylar ramus was filled with chondrocytes, except the inferior area, in which there were red bone cells (Appendix Fig. 1a). By E18.5, the bone collar was expanded upward with a dramatic reduction of cartilage area (Appendix Fig. 1c).

Taken together, the cell lineage–tracing studies and the ex vivo condylar cartilage culture data support the new concept that chondrocytes directly transform into bone cells in MCC bone formation. The cell lineage–tracing technique not only maps subchondral bone cell origins but also identifies the initial ossification site of endochondral bone in the inferior portion of MCC and indicates the direction in which ossification proceeds during the late developmental stages.

Discussion

Our results argue strongly against the idea that endochondral bone formation in the mandibular condyle occurs via a process that involves significant cell death by HCs or inmigration of cells from bone marrow (Fig. 5a). We found that although some HCs undergo apoptosis, collectively they express high levels of the antiapoptotic protein Bcl2. In addition, immunoreactivity for ALP is strong in HCs, and surprisingly, some undergo cell division. Thus, MCC HCs resemble metabolically active cells that secrete a marker for bone cells rather than inert, metabolically inactive cells waiting to undergo apoptosis.

The use of cell lineage–tracing enabled us to dissect this question in a much more definitive way. These studies demonstrate that the transformation of chondrocytes, in particular HCs, into bone cells is responsible for the majority of bone cells in the trabecular bone underlying the MCC. A time course study of the condyle at days 1, 2, 8, and 14 after tamoxifen injection in 2-wk-old mice showed a gradual increase of red bone cells in the subchondral bone (Appendix Fig. 4), further supporting the concept of the direct transformation of chondrocytes into bone cells. In newborn mice, these cartilage-derived bone cells fluoresced red in superimposed images of red and green, presumably because the cells had not yet begun to secrete a sufficient amount of Col1 (green fluorescence) to appear yellow in superimposed images. By P10 and at subsequent ages, only those cells in the bone relatively close to the cartilage-bone interface exhibited red fluorescence, while a great majority of the cells in deeper layers fluoresced yellow. Yet, some of these red cells could be osteocytes, as many osteocytes express low or extremely low *Col1*, as shown by a lack of detection of *Col1* signals in osteocytes by in situ hybridization in condylar ramus (Appendix Fig. 3). Moreover, the red color is more readily sensed than green color.

Yellow-fluorescing cells were also common in the cortical bone of the condylar neck at P10 and after. In limb cartilage, the percentage of HC-derived cells that become osteoblasts or osteocytes has been estimated at anywhere from 20% to 30% or 60% to 70% (Zhou et al. 2014) to 80% (L. Yang et

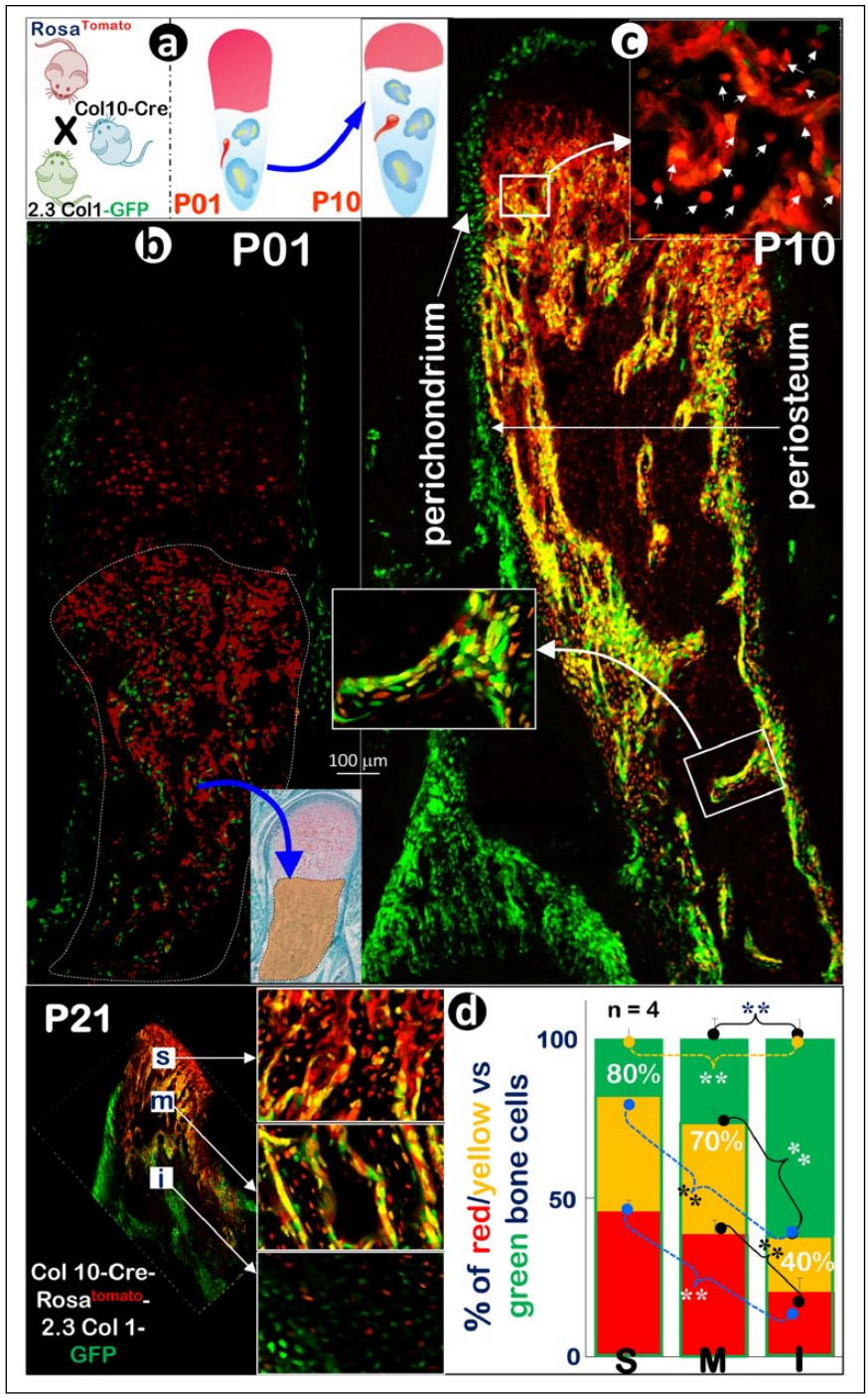

Figure 4. Qualitative and quantitative documentation of direct transformation of the initial condylar cartilage template into bone in *Col10-Cre, 2.3Col1-GFP*, and *ROSA-*^{tdTomato} triple transgenic mice. (**a**) A cartoon illustrates the cross that generates triple mice containing *Col10-Cre, ROSA-*^{tdTomato}, and 2.3 *Col*1-GFP (left), and it depicts the hypothesis of direct transformation of the early condylar cartilage template into bone from the inferior area upward (right). (**b**) The merged P01 (postnatal day 1) confocal image revealed green bone cells in perichondrium and periosteum on the periphery, red cartilage cells in the top center, and mixed red/yellow/green bone cells in the lower center. The safranin O–stained image from the adjacent section reflects this direct transformation of cartilage to bone starting from lower region (right lower corner). (**c**) The P10 confocal image showed a mix of different-colored bone cells in the subchondral bone (white arrows; top center and the enlarged inset on top right), bone marrow (containing red bone marrow cells), trabecular bone (the enlarged insert on left), and periosteum. (**d**) The low-magnification confocal image in the lower left panel illustrates the 3 areas for quantitation of bone cell origin: yellow/red derived from chondrocytes and green originating from nonchondrocyte progenitor cells at P21. The enlarged representative confocal images that were used for quantitation in each area (superior, s; mid, m; inferior, i) are shown on the lower middle panel. The total cell numbers in each area were approximately 500. The statistical analysis of differences in red, yellow, and green cells among the 3 regions is presented in the lower right panel ($n = 4$; $^{**}P < 0.01$).

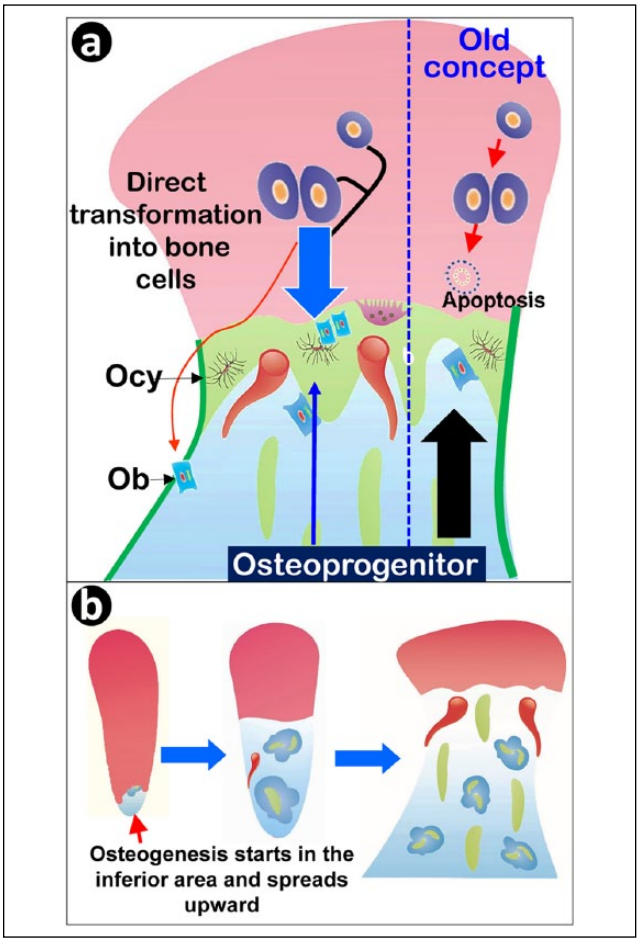

Figure 5. Cartoon depictions of our working hypotheses concerning the direct transformation of chondrocytes into bone cells and the initial locus of this area of ossification in the mandibular condyle. (**a**) Our working hypothesis is that the embryonic condylar chondrocytes, instead of undergoing apoptosis, directly transform into bone cells in the superior (~80%), middle (~70%), and inferior (40%) condylar center regions, plus some in the periosteal membrane. This view challenges the old concept that most chondrocytes undergo apoptosis prior to bone formation. (**b**) The initial direct transformation starts from the inferior area of the cartilage and gradually expands upward as the cartilage becomes thinner but continues to grow via proliferation in the prechondroblastic zone. Ob, osteoblasts; Ocy, osteocytes.

al. 2014). Our quantitative data fit within the high end of this spectrum, suggesting that around 80% of bone cells within the bone near the cartilage-bone interface are cartilage derived. However, our approach of quantifying successively deeper regions of the condylar neck allowed us to characterize a gradient of bone cell derivation, in which 80% of bone cells are cartilage derived in the immediately subchondral (superior) zone, 70% in the next deeper (middle) zone, and only 40% in the deepest (inferior) zone. While 60% of bone cells in the inferior zone are indeed derived from nonchondrocyte-derived bone progenitor cells, even this fraction challenges the traditional view about endochondral bone formation.

In this study, we also propose that the MCC cartilage is a 1-sided version of the primary ossification center of the long bone, even though growth occurs at only 1 end (the inferior; Fig. 4a). However, no secondary ossification center forms as in long bone. Alternately, the MCC may resemble an incompletely ossified fracture callus, which has been shown to ossify largely from cartilage-derived bone (Zhou et al. 2014).

Other investigations by our laboratory have highlighted the virtual cessation of endochondral bone formation in postnatal, actively growing mice with a conditional knockout in cartilage of a growth factor receptor (BMPr1a; Jing et al. 2013; Jing, Hinton, Mishina, et al. 2014) or a transcription factor (osterix; Jing, Hinton, Jing, et al. 2014). Those results echo the principal conclusion of this study—that a majority of endochondrally formed bone is regulated by transformation of cells from the overlying cartilage. Thus, a change in gene expression that drastically downregulates chondrogenesis (as in *BMPr1a* and *Osx* cKO mice) can effect major deficits in subchondral bone formation. This opens up a new possibility: regulation of bone formation via agents that act on cartilage.

Our findings agree with studies in limb growth plate, even though the secondary fibrocartilaginous MCC differs considerably from the growth plate in its developmental origin. This agreement is particularly important to the field, as cartilages of very disparate origins appear to share a common and pervasive mechanism involving transformation of chondrocytes directly into bone cells. With the burgeoning number of studies in long bone and in condylar cartilage, the idea that HCs can transform into osteoblasts and osteocytes has gained momentum and credence. Given the likelihood that transformation of HCs accounts for the majority of subchondral trabecular bone cells, this concept, once at odds with the prevailing paradigm of endochondral bone formation, seems to be becoming the new paradigm. Taken in conjunction with the unexpected finding that some HCs in the MCC (Fig. 1) and growth plate (Enishi et al. 2014; Zhou et al. 2014) undergo cell division, this hints at a surprising functional plasticity for HCs. While the environmental cues and regulators of these changes are not now understood, the possibilities are tantalizing.

In summary, this study presents convincing evidence that direct transformation of HCs into bone cells, rather than the old concept of HC apoptosis followed by bone marrow cell invasion, is the most important physiologic mechanism underlying endochondral bone formation. Moreover, our quantitative data indicate that this process is responsible for the majority of bone cells, making chondrocytes crucially important for normal endochondral bone formation. Finally, our studies revealed an ossification site in the inferior region of the condylar cartilage during endochondral bone formation (Fig. 5b), which is different from the ossification site during mandibular membranous bone formation (Nanci 2007).

Author Contributions

Y. Jing, contributed to conception, design, data acquisition, analysis, and interpretation, drafted and critically revised the manuscript; X. Zhou, K. von der Mark, B. de Crombrugghe, contributed to design and data acquisition, drafted and critically revised the manuscript; X. Han, J. Jing, J. Wang, contributed to design and

data analysis, drafted and critically revised the manuscript; R.J. Hinton, J.Q. Feng, contributed to conception, design, and data interpretation, drafted and critically revised the manuscript. All authors gave final approval and agree to be accountable for all aspects of the work.

Acknowledgments

This study was partially supported by National Institutes of Health grants DE025014 and R56DE022789 to J.Q.F. and by National Natural Science Foundation of China grant 81371172 to X.H. The authors declare no potential conflicts of interest with respect to the authorship and/or publication of this article.

References

Akiyama H, Kim JE, Nakashima K, Balmes G, Iwai N, Deng JM, Zhang Z, Martin JF, Behringer RR, Nakamura T, et al. 2005. Osteo-chondroprogenitor cells are derived from Sox9 expressing precursors. Proc Natl Acad Sci U S A. 102(41):14665–14670.

Enishi T, Yukata K, Takahashi M, Sato R, Sairyo K, Yasui N. 2014. Hypertrophic chondrocytes in the rabbit growth plate can proliferate and differentiate into osteogenic cells when capillary invasion is interposed by a membrane filter. PloS One. 9(8):e104638.

Feng JQ, Clark NB. 1994. Renal responses to parathyroid hormone in young chickens. Am J Physiol. 267(1 Pt 2):R295–R302.

Gebhard S, Hattori T, Bauer E, Schlund B, Bosl MR, de Crombrugghe B, von der Mark K. 2008. Specific expression of Cre recombinase in hypertrophic cartilage under the control of a BAC-Col10a1 promoter. Matrix Biol. 27(8):693–699.

Gibson G. 1998. Active role of chondrocyte apoptosis in endochondral ossification. Microsc Res Tech. 43(2):191–204.

Henry SP, Jang CW, Deng JM, Zhang Z, Behringer RR, de Crombrugghe B. 2009. Generation of aggrecan-CreERT2 knockin mice for inducible Cre activity in adult cartilage. Genesis. 47(12):805–814.

Jiang X, Kalajzic Z, Maye P, Braut A, Bellizzi J, Mina M, Rowe DW. 2005. Histological analysis of GFP expression in murine bone. J Histochem Cytochem. 53(5):593–602.

Jing J, Hinton RJ, Jing Y, Liu Y, Zhou X, Feng JQ. 2014. Osterix couples chondrogenesis and osteogenesis in post-natal condylar growth. J Dent Res. 93(10):1014–1021.

Jing J, Hinton RJ, Mishina Y, Liu Y, Zhou X, Feng JQ. 2014. Critical role of Bmpr1a in mandibular condyle growth. Connect Tissue Res. 55 Suppl 1:73–78.

Jing J, Ren Y, Zong Z, Liu C, Kamiya N, Mishina Y, Liu Y, Zhou X, Feng JQ. 2013. BMP receptor 1A determines the cell fate of the postnatal growth plate. Int J Biol Sci. 9(9):895–906.

Kahn AJ, Simmons DJ. 1977. Chondrocyte-to-osteocyte transformation in grafts of perichondrium-free epiphyseal cartilage. Clin Orthop Relat Res. 129:299–304.

Kalajzic Z, Liu P, Kalajzic I, Du Z, Braut A, Mina M, Canalis E, Rowe DW. 2002. Directing the expression of a green fluorescent protein transgene in differentiated osteoblasts: comparison between rat type I collagen and rat osteocalcin promoters. Bone. 31(6):654–660.

Kronenberg HM. 2003. Developmental regulation of the growth plate. Nature. 423(6937):332–336.

Luder HU, Leblond CP, von der Mark K. 1988. Cellular stages in cartilage formation as revealed by morphometry, radioautography and type II collagen immunostaining of the mandibular condyle from weanling rats. Am J Anat. 182(3):197–214.

Nanci A. 2007. Ten Cate's oral histology : development, structure, and function. 7th. St. Louis, MO: Mosby.

Ono N, Ono W, Nagasawa T, Kronenberg HM. 2014. A subset of chondrogenic cells provides early mesenchymal progenitors in growing bones. Nat Cell Biol. 16(12):1157–1167.

Richardson M, Singh G. 2003. Observations on the use of the avian chorioallantoic membrane (CAM) model in investigations into angiogenesis. Curr Drug Targets Cardiovasc Haematol Disord. 3(2):155–185.

Roach HI. 1992. Trans-differentiation of hypertrophic chondrocytes into cells capable of producing a mineralized bone matrix. Bone Miner. 19(1):1–20.

Silbermann M, Reddi AH, Hand AR, Leapman RD, Von der Mark K, Franzen A. 1987. Further characterisation of the extracellular matrix in the mandibular condyle in neonatal mice. J Anat. 151:169–188.

Yang G, Zhu L, Hou N, Lan Y, Wu XM, Zhou B, Teng Y, Yang X. 2014. Osteogenic fate of hypertrophic chondrocytes. Cell Res. 24(10):1266–1269.

Yang L, Tsang KY, Tang HC, Chan D, Cheah KS. 2014. Hypertrophic chondrocytes can become osteoblasts and osteocytes in endochondral bone formation. Proc Natl Acad Sci U S A. 111(33):12097–12102.

Zhai Y, Kuick R, Nan B, Ota I, Weiss SJ, Trimble CL, Fearon ER, Cho KR. 2007. Gene expression analysis of preinvasive and invasive cervical squamous cell carcinomas identifies HOXC10 as a key mediator of invasion. Cancer Res. 67(21):10163–10172.

Zhang R, Lu Y, Ye L, Yuan B, Yu S, Qin C, Xie Y, Gao T, Drezner MK, Bonewald LF, et al. 2011. Unique roles of phosphorus in endochondral bone formation and osteocyte maturation. J Bone Miner Res. 26(5):1047–1056.

Zhou X, von der Mark K, Henry S, Norton W, Adams H, de Crombrugghe B. 2014. Chondrocytes transdifferentiate into osteoblasts in endochondral bone during development, postnatal growth and fracture healing in mice. PLoS Genet. 10(12):e1004820.